

# An analytic treatment of Quartic Hilltop Inflation

Konstantinos Dimopoulos<sup>1</sup>

*Consortium for Fundamental Physics  
Physics Department, Lancaster University  
Lancaster, LA1 4YB, UK*

## Abstract

Quartic hilltop inflation remains one of the most successful inflationary models. Yet, the expectations of early treatments of hilltop inflation would contradict the observations and render the model excluded. However, recent numerical treatment has demonstrated that quartic hilltop inflation actually fares well with observations. In this work, a fully analytic treatment of the model aims to dispel the mystery surrounding the behaviour of quartic hilltop inflation. The results obtained are in excellent agreement with numerical works on the subject, yet offer simple analytic formulas to calculate observables and easily test thereby quartic hilltop inflation, hopefully revealing information on the theoretical background.

The precision of cosmological observations in the last few years has grown so high that the paradigm of inflation model-building is changed. Out are the simple monomial chaotic models while centre-stage is reserved for plateau models. Yet, in contrast to the large-field plateau models, hilltop inflation, a small field family of models, seems to be doing well. However, based only on the early expectations we would expect the model to be another failure. What allows hilltop inflation to escape the fate of monomial chaotic models?

The term hilltop inflation was coined by Boubekeur and Lyth in 2005 [1] but the model was known well before, as far back as new inflation [2]. The potential density of the model is

$$V(\phi) = V_0 \left[ 1 - \lambda \left( \frac{\phi}{m_P} \right)^q \right] + \dots, \quad (1)$$

where  $\phi$  is the inflaton field,  $V_0$  is a constant density scale,  $\lambda$  some parameter,  $q > 0$  is typically an integer, the ellipsis denotes higher order terms which stabilise the potential and  $m_P = (8\pi G)^{-1/2}$  is the reduced Planck mass with  $G$  being Newton's gravitational constant. Early analytic treatment of the model suggested that the spectral index of the curvature perturbation is [3]

$$n_s = 1 - 2 \left( \frac{q-1}{q-2} \right) \frac{1}{N}, \quad (2)$$

where  $N$  is the remaining e-folds of inflation when the cosmological scales exit the horizon.

Arguably, one of the most motivated members of the family of hilltop inflation models is quartic hilltop inflation, where  $q = 4$ . Thus, in the case of quartic hilltop inflation we would expect

$$n_s = 1 - \frac{3}{N}, \quad (3)$$

Taking  $N = 60$ , the above gives  $n_s = 0.95$ , which is much too low to be acceptable. The number of e-folds can decrease if there is a period of effective matter domination after inflation, but this makes the spectrum even redder. One can obtain the desired value  $n_s \gtrsim 0.96$  only when  $N \gtrsim 75$ , which is way too large.<sup>2</sup> Thus, we are tempted to conclude that quartic hilltop inflation is excluded.

However, in recent years it was gradually realised that actually hilltop inflation fares well with observations. In fact, quartic hilltop inflation is one of the models selected by the Planck Collaboration to feature in their main graph (see Fig. 1). The model has been carefully looked into in *Encyclopædia Inflationaris* [5], whose results are being used by the Planck Collaboration. However, the treatment was largely numerical and one might say obscure. It was not clear why the model departs from the early expectations described above. A more recent work [6] has made

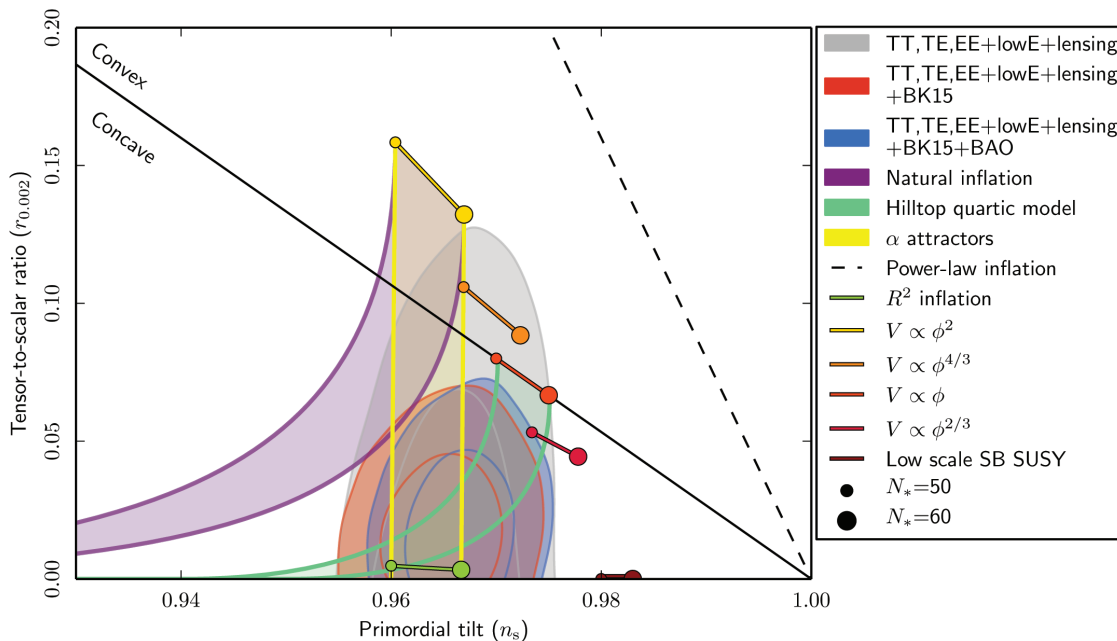


Figure 1: Diagram in the  $n_s - r$  plane featuring the Planck 2018 data contrasted with the predictions of some prominent inflation models. The predictions of quartic hilltop inflation are shown with cyan convex curves (see legend). It can be seen that the model is successful as there is significant overlap with the allowed parameter space. Figure taken from Ref. [4].

an effort to peer into the physical interpretation of the behaviour of hilltop inflation, found in Ref. [5]. However, this too is a numerical investigation.

It can be argued that numerical investigation, while it can reveal unexpected behaviour, which was previously not realised, is in itself rather opaque, the computer being akin to a black box. In contrast, the clarity of analytic calculation is unparalleled. We already know *what* should come out now, thanks to the numerical treatment. In this work, we look into the *why* quartic inflation behaves as such.

The result in Eq. (3) (and Eq. (2)) is based on two crucial assumptions. One is that the expectation value of the inflaton field  $N$  e-folds before the end of inflation is much smaller than its vacuum expectation value (VEV), i.e.  $\phi(N) \ll \langle \phi \rangle \sim m_P/\lambda^{1/q}$  (with  $q = 4$ ), such that during inflation  $V(\phi) \simeq V_0$ . The other assumption is that the contribution of the value of the inflaton  $\phi_{\text{end}}$  when inflation ends is negligible and disregarded in the calculation of  $N(\phi)$  (which is the inverse of  $\phi(N)$ ). It turns out that both these assumptions are unwarranted. Below we analytically calculate the spectral index  $n_s$  and the tensor to scalar ratio  $r$ , which are the main observables that an inflationary model generates, considering  $\phi \lesssim \langle \phi \rangle$  so the influence of the inflaton to the potential density is not disregarded during inflation. Similarly, the influence of  $\phi_{\text{end}}$  to the value of  $N(\phi)$  is retained. The latter effect is crucial because, as shown below, when  $\lambda \ll 1$  we have  $N \rightarrow N + 1/4\sqrt{\lambda}$ , which can become significantly larger than 60.

The quartic hilltop inflation model is:

$$V(\phi) = V_0 \left[ 1 - \lambda \left( \frac{\phi}{m_P} \right)^4 \right] + \dots, \quad (4)$$

where the ellipsis denotes higher order terms which stabilise the potential. They become important

<sup>1</sup>k.dimopoulos1@lancaster.ac.uk

<sup>2</sup>Even with a subsequent period of kination, lasting until the electroweak scale,  $N$  cannot grow larger than 67.

only when the inflaton reaches its VEV; not during inflation, so we disregard them from now on (but see later).

From the above, we have

$$V' = -4\lambda \frac{V_0}{m_P} \left( \frac{\phi}{m_P} \right)^3 \quad (5)$$

$$\text{and } V'' = -12\lambda \frac{V_0}{m_P^2} \left( \frac{\phi}{m_P} \right)^2. \quad (6)$$

Using these, we find the slow-roll parameters

$$\varepsilon = \frac{1}{2} m_P^2 \left( \frac{V'}{V} \right)^2 = \frac{8\lambda^2 \left( \frac{\phi}{m_P} \right)^6}{\left[ 1 - \lambda \left( \frac{\phi}{m_P} \right)^4 \right]^2} \quad (7)$$

$$\text{and } \eta = m_P^2 \frac{V''}{V} = -\frac{12\lambda \left( \frac{\phi}{m_P} \right)^2}{1 - \lambda \left( \frac{\phi}{m_P} \right)^4} < 0. \quad (8)$$

Connecting the inflaton value with the remaining e-folds of inflation, we find

$$N = \frac{1}{m_P^2} \int_{\phi_{\text{end}}}^{\phi^{(N)}} \frac{V d\phi}{V'} \Rightarrow \bar{N} \equiv N + N_{\text{end}} = \frac{1}{8\lambda} \left[ \left( \frac{\phi}{m_P} \right)^{-2} + \lambda \left( \frac{\phi}{m_P} \right)^2 \right] \quad (9)$$

$$\Rightarrow \left( \frac{\phi}{m_P} \right)^2 = 4\bar{N}[Z], \quad (10)$$

where

$$[Z] \equiv 1 - \sqrt{1 - \frac{1}{Z}} > 0, \quad (11)$$

with

$$Z \equiv 16\lambda \bar{N}^2 > 0. \quad (12)$$

In the above, we have defined

$$N_{\text{end}} \equiv \frac{1}{8\lambda} \left[ \left( \frac{\phi_{\text{end}}}{m_P} \right)^{-2} + \lambda \left( \frac{\phi_{\text{end}}}{m_P} \right)^2 \right]. \quad (13)$$

Let us estimate  $N_{\text{end}}$ . There are two possibilities, which have to do with which slow-roll parameter is responsible for the termination of inflation:

**Case A:**  $|\eta(\phi_{\text{end}})| = 1$

From Eq. (8), we find

$$\left( \frac{\phi_{\text{end}}}{m_P} \right)^4 + 12 \left( \frac{\phi_{\text{end}}}{m_P} \right)^2 - \frac{1}{\lambda} = 0, \quad (14)$$

which has only one acceptable solution

$$\left( \frac{\phi_{\text{end}}}{m_P} \right)^2 = 6 \left( \sqrt{1 + \frac{1}{36\lambda}} - 1 \right). \quad (15)$$

Using this in Eq. (13), we obtain

$$N_{\text{end}} = \frac{1}{8\lambda} \left[ \frac{1}{6} \left( \sqrt{1 + \frac{1}{36\lambda}} - 1 \right)^{-1} + 6\lambda \left( \sqrt{1 + \frac{1}{36\lambda}} - 1 \right) \right]. \quad (16)$$

The above exact result is reduced to the limits

$$N_{\text{end}} \simeq \begin{cases} \frac{1}{4\sqrt{\lambda}} & \text{when } \lambda \ll 1 \\ \frac{3}{2} & \text{when } \lambda \gg 1 \end{cases}. \quad (17)$$

**Case B:**  $\varepsilon(\phi_{\text{end}}) = 1$

From Eq. (7), we find

$$\left[ \left( \frac{\phi_{\text{end}}}{m_P} \right) + 2\sqrt{2} \right] \left( \frac{\phi_{\text{end}}}{m_P} \right)^3 = \frac{1}{\lambda}. \quad (18)$$

This is impossible to solve analytically. However, we can still consider the limiting values of  $\lambda$ . Indeed, if  $\lambda \ll 1$  then we have  $\phi_{\text{end}} \gg m_P$  and the above equation gives

$$\left( \frac{\phi_{\text{end}}}{m_P} \right)^2 = \frac{1}{\sqrt{\lambda}}. \quad (19)$$

Inserting this in Eq. (13) we find  $N_{\text{end}} = 1/4\sqrt{\lambda}$ . In the opposite limit  $\lambda \gg 1$  we have  $\phi_{\text{end}} \ll m_P$  and Eq. (18) becomes

$$\left( \frac{\phi_{\text{end}}}{m_P} \right)^3 = \frac{1}{2\sqrt{2}\lambda}. \quad (20)$$

Inserting this in Eq. (13) we obtain  $N_{\text{end}} = 1/4\lambda^{1/3} < 1$ .

Thus, in general we have

$$N_{\text{end}} \simeq \begin{cases} \frac{1}{4\sqrt{\lambda}} & \text{when } \lambda \ll 1 \\ \frac{1}{4\lambda^{1/3}} < 1 & \text{when } \lambda \gg 1 \end{cases}. \quad (21)$$

In overall, no matter which slow-roll parameter is taken to end inflation, we have found that  $N_{\text{end}} \lesssim 1$  when  $\lambda \gg 1$  and

$$N_{\text{end}} = \frac{1}{4\sqrt{\lambda}} \quad \text{when } 0 < \lambda \ll 1. \quad (22)$$

Thus, we see that when  $\lambda \gg 1$  the contribution of  $N_{\text{end}}$  to  $\bar{N}$  is negligible so that  $\bar{N} \simeq N$ . As we show below, this is unacceptable so the only possibility is  $\lambda \ll 1$  for which

$$\bar{N} = N + \frac{1}{4\sqrt{\lambda}}. \quad (23)$$

To find the observational requirements on the value of  $\lambda$  we need to calculate the spectral index of the generated primordial curvature perturbation. For the spectral index we have

$$n_s = 1 - 6\varepsilon + 2\eta = 1 - 2|\eta| \left( 1 + 3\frac{\varepsilon}{|\eta|} \right). \quad (24)$$

From Eqs. (8) and (10), we find

$$2|\eta| = \frac{3}{\bar{N}} \frac{Z[Z]}{1 - Z[Z]}. \quad (25)$$

Similarly, using Eqs. (7) and (10) we obtain

$$3\frac{\varepsilon}{|\eta|} = \frac{2Z[Z] - 1}{1 - Z[Z]} \Rightarrow 1 + 3\frac{\varepsilon}{|\eta|} = \frac{Z[Z]}{1 - Z[Z]}, \quad (26)$$

where we used that

$$1 - \lambda \left( \frac{\phi}{m_P} \right)^4 = 2(1 - Z[Z]). \quad (27)$$

Combining Eqs. (24), (25) and (26), we find

$$n_s = 1 - \frac{3}{\bar{N}} \left( \frac{Z[Z]}{1 - Z[Z]} \right)^2. \quad (28)$$

The above reduces to  $n_s = 1 - 3/\bar{N}$  in the limit  $Z \gg 1$ . Disregarding also  $N_{\text{end}}$  we obtain Eq. (3). This reveals the influence of considering  $\phi \lesssim \langle \phi \rangle$  (corresponding to  $Z \gtrsim 1$ ) compared to  $\phi \ll \langle \phi \rangle$  (corresponding to  $Z \gg 1$ ), which was assumed in Ref. [3].

Recasting Eq. (28), we find

$$\frac{\bar{N}}{3}(1 - n_s) = \left( \frac{Z[Z]}{1 - Z[Z]} \right)^2 = \left( \frac{1}{\sqrt{1 - \frac{1}{Z}}} \right)^2 = \frac{Z}{Z - 1} \quad (29)$$

Thus, in view of Eq. (12), we obtain

$$16\lambda\bar{N}^2 = Z = \frac{\bar{N}(1 - n_s)}{\bar{N}(1 - n_s) - 3}. \quad (30)$$

Note that the above requires that  $\bar{N}(1 - n_s) > 3$  so that  $Z > 0$ . If  $\lambda \gg 1$  then  $\bar{N} \simeq N$  and the requirement becomes  $n_s \leq 1 - 3/N$ . For  $N \leq 60$  we find  $n_s \leq 0.95$ , which is observationally excluded. Therefore, we must have  $\lambda \ll 1$ . In this case  $\bar{N}$  is given by Eq. (23).

Using Eqs. (12), (23) and (30), we find

$$\sqrt{\lambda} = \frac{2(1 - n_s)N - 3}{4N[3 - (1 - n_s)N]} \Rightarrow \mu \equiv m_P/\lambda^{1/4} = \left\{ \frac{4N[3 - (1 - n_s)N]}{2(1 - n_s)N - 3} \right\}^{1/2} m_P, \quad (31)$$

where  $\mu \sim \langle \phi \rangle$  is the inflaton VEV. This is valid only when  $\frac{3}{2} < N(1 - n_s) < 3$ , because  $\sqrt{\lambda} > 0$ . Considering the range  $N = 50 - 60$  the observations for the spectral index ( $n_s = 0.965 \pm 0.004$  for negligible tensors [4]) suggest that  $\lambda \lesssim 10^{-4}$ . This means that the VEV of the inflaton is super-Planckian  $\langle \phi \rangle \sim m_P/\lambda^{1/4} \gtrsim 10 m_P$ , which undermines the perturbative origin of the potential. Values of  $\lambda(n_s)$  for a given choice of  $N$  are shown in Fig. 2.

Let us discuss the tensor to scalar ratio now. Using Eqs. (7), (10) and (27), we can write

$$r = 16\varepsilon = \frac{128\lambda^2 \left(\frac{\phi}{m_P}\right)^6}{\left[1 - \lambda\left(\frac{\phi}{m_P}\right)^4\right]^2} = \frac{128\lambda^2 (4\bar{N}[Z])^3}{[2(1 - Z[Z])]^2}. \quad (32)$$

Combining this with Eq. (29), we have

$$r = \frac{32\lambda^2 (4\bar{N})^3 [Z]}{(1 - \frac{1}{Z})Z^2} = \frac{8}{\bar{N}} \frac{Z[Z]}{Z - 1} = \frac{8}{3}(1 - n_s)[Z], \quad (33)$$

where we also used Eq. (12). Employing the definition of  $[Z]$  in Eq. (11) and Eq. (29) again, we end up with

$$r = \frac{8}{3}(1 - n_s) \left[ 1 - \frac{\sqrt{3}}{\sqrt{(1 - n_s)\bar{N}}} \right]. \quad (34)$$

Because  $r > 0$  and the spectrum is red, we expect the expression in the square brackets in the above to be positive. Using Eq. (23) and after a little algebra, this requirement becomes the bound  $\sqrt{\lambda} < \frac{1}{4} \left( \frac{3}{1 - n_s} - N \right)^{-1}$ . In view of Eq. (31), this bound amounts to  $n_s > 1 - \frac{9}{2\bar{N}}$ , which is satisfied for  $N = 50 - 60$  and the observed values of  $n_s$ .

Using Eqs. (9) and (31), we can recast Eq. (34) as

$$r = \frac{8}{3}(1 - n_s) \left\{ 1 - \frac{\sqrt{3[2(1 - n_s)N - 3]}}{(1 - n_s)N} \right\}. \quad (35)$$

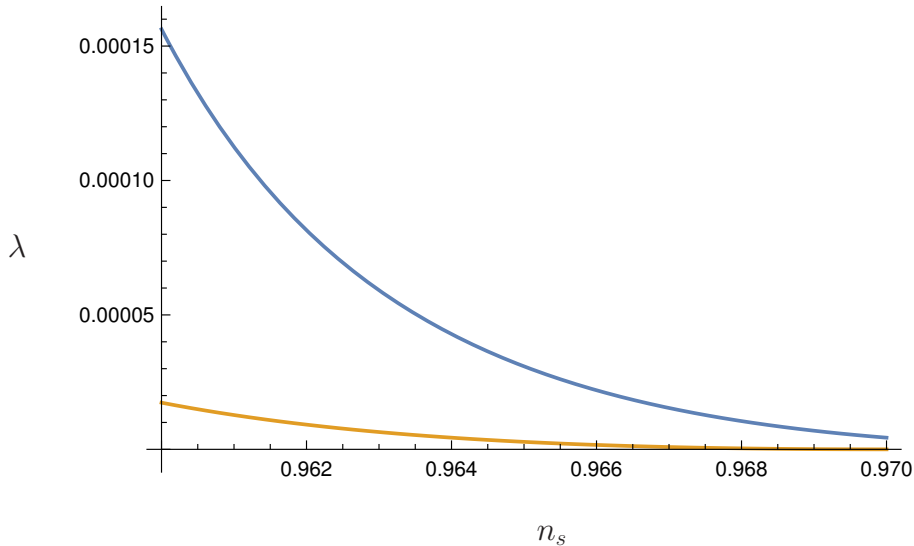


Figure 2: The value of  $\lambda$  as a function of  $n_s$  in the range of interest  $n_s \in [0.960, 0.970]$  for different values of  $N$  according to Eq. (31):  $N = 60$  in the upper curve (blue) and  $N = 50$  in the lower curve (orange). It can be seen that, when  $N = 50 - 60$  we have  $\lambda \lesssim 10^{-4}$  in the range of interest for  $n_s$ . This means that the VEV  $\langle \phi \rangle \sim m_P / \lambda^{1/4} \gtrsim 10 m_P$  is mildly super-Planckian.

For typical values  $N = 60$  and  $n_s = 0.965$  the above suggests  $r = 0.0446$ , which will be observable in the near future. Contrasting the above with observations reproduces the analysis of the Planck Collaboration, as can be seen by comparing Fig. 1 with Fig. 3.

It is interesting that the limiting values of  $r(n_s)$  correspond to the predictions of linear inflation, with  $V(\phi) \propto \phi$ . Indeed, linear inflation suggests  $n_s = 1 - \frac{3}{2N}$ . Inserting this value in Eq. (35) one obtains  $r = \frac{4}{N}$ , which is the prediction of linear inflation. This has been noticed for some time but it is nice to confirm it analytically here. In fact, in Ref. [5] it is shown that this limit is attained by all hilltop models of the form in Eq. (1) with any  $q > 0$ . The issue was recently explored in Ref. [6], who argued that hilltop potentials approximate linearity when  $V \rightarrow 0$  and the potential is about to become negative unless stabilised by higher order terms implied by the ellipsis in Eqs. (1) and (4). But these terms would deform the potential near the VEV, rendering the form of the potential different from linear. Therefore, the authors of Ref. [6] argue that the approach to the linear inflation predictions in Fig. 3 is not to be trusted. How far from this are the predictions of the model trustworthy depends on the stabilising terms of the potential.

Finally, let us enforce the COBE constraint to estimate  $V_0$  in the potential, such that the model generates the correct magnitude of the curvature perturbation. In slow-roll inflation we have

$$\sqrt{\mathcal{P}_\zeta} = \frac{1}{2\sqrt{3}\pi} \frac{V^{3/2}}{m_P^3 |V'|} = \frac{1}{8\sqrt{3}\pi\lambda} \frac{\sqrt{V_0}}{m_P^2} \frac{\left[1 - \lambda \left(\frac{\phi}{m_P}\right)^4\right]^{3/2}}{\left(\frac{\phi}{m_P}\right)^3} = \frac{\sqrt{2}}{32\sqrt{3}\pi\lambda} \frac{\sqrt{V_0}}{m_P^2} \left(\frac{1 - Z[Z]}{N[Z]}\right)^{3/2}, \quad (36)$$

where we used Eqs. (4) and (5) and then Eqs. (10) and (27). In view of Eqs. (11), (12) and (29), we can write

$$\frac{1 - Z[Z]}{N[Z]} = 16\lambda \left(\frac{3\bar{N}}{1 - n_s}\right)^{1/2}. \quad (37)$$

Combining the above with Eq. (36) we find

$$\frac{V_0}{m_P^4} = \frac{3\pi^2 \mathcal{P}_\zeta}{8\lambda} \left(\frac{1 - n_s}{3\bar{N}}\right)^{3/2}. \quad (38)$$

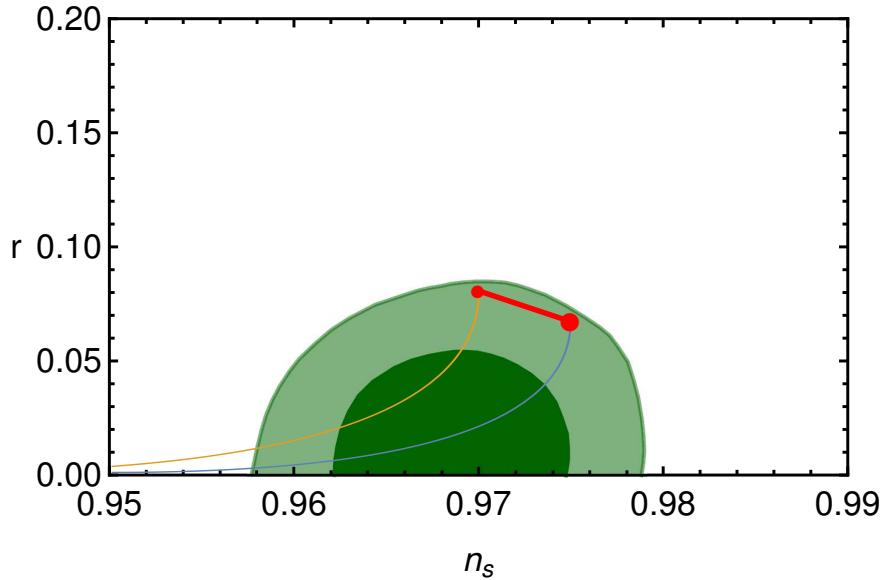


Figure 3: The predictions of quartic hilltop inflation for selected values of  $N$  according to Eq. (35):  $N = 60$  in the lower curve (blue) and  $N = 50$  in the upper curve (orange), contrasted with the observational data of Planck 2015. Values of  $N \in (50, 60)$  correspond to the band between the above curves. The band is capped at the slanted solid line (red) which depicts the predictions of linear inflation.

Taking the values  $\mathcal{P}_\zeta = 2.1 \times 10^{-9}$  and  $n_s \simeq 0.965$  with  $\lambda \simeq 10^{-4}$  and  $N = 60$  (so  $\bar{N} \simeq 85$ , cf. Eq. (9)) we find  $V_0^{1/4} \sim 10^{16}$  GeV, which is the GUT-scale as expected.

This concludes our analytical study of quartic hilltop inflation. Our main results are the expressions in Eqs. (31) and (35). The latter is shown to reproduce exactly the numerical results, as can be seen in Fig. 3. We found that, for quartic hilltop inflation to work we need a mildly super-Planckian VEV of order  $\langle \phi \rangle \gtrsim 10 m_P$ . A sub-Planckian VEV results in the traditional expression in Eq. (3), which is ruled out as it gives rise to  $n_s \lesssim 0.95$ . The performance of the model, when the VEV is super-Planckian, is crucially determined by the contribution of the value  $\phi_{\text{end}}$  of the inflaton when inflation is terminated, which can add significantly to the number of e-folds which correspond to the cosmological scales, as demonstrated by Eq. (9). It has to be noted that the predictions of the model are not trustworthy when approaching the results of linear inflation (see Fig. 3) because the effect of the stabilising terms in the potential cannot be ignored then. However, this limit is already disfavoured by observations (see Fig. 1).

After this work came out, it was realised that some analytic treatment of quartic hilltop inflation is also done in Ref. [7]. The author obtains a parametric expression of  $r(n_s)$ , which is arguably not as straightforward as Eq. (35).

I would like to thank David Sloan for discussions. KD was supported (in part) by the Lancaster-Manchester-Sheffield Consortium for Fundamental Physics under STFC grant: ST/L000520/1.

## References

- [1] L. Boubekeur and D. H. Lyth, JCAP **07** (2005), 010.
- [2] A. D. Linde, Phys. Lett. B **116** (1982), 335-339.
- [3] D. H. Lyth and A. Riotto, Phys. Rept. **314** (1999), 1-146.
- [4] Y. Akrami *et al.* [Planck], [arXiv:1807.06211 [astro-ph.CO]].

- [5] J. Martin, C. Ringeval and V. Vennin, *Phys. Dark Univ.* **5-6** (2014), 75-235.
- [6] R. Kallosh and A. Linde, *JCAP* **09** (2019), 030.
- [7] C. M. Lin, *JCAP* **06** (2020), 015.